第 22 卷第 6 期
2003 年 12 月

红外与毫米波学报
J. Infrared Millim. Waves

Vol. 22, No. 6
December, 2003

A NEW GEOMETRIC ACTIVE CONTOUR FOR MEDICAL IMAGE SEGMENTATION *

CEN Feng QI Fei-Hu

(Department of Computer Science & Engineering, Shanghai Jiaotong University, Shanghai 200030, China)

Abstract Generally, the segmentation of a medical image is difficult, because the medical image is often corrupted by norrupted by noise, and the anatomical shape in the medical image is complicated. In this paper presents a new geometric active contour scheme for medical image segmentation. First, we regularize the attraction force field in the geometric active contour model to extend the capture range of the object boundaries, and improve the ability of convergence to the concavities. Then, using a multi-scale scheme improve the boundary detection accuracy. In addition, combining the regularization and the multi-scale method, the proposed scheme can effectively suppress and eliminate the noise and the spurious edges in the medical images. Furthermore, the topology of the deforming curve can naturally change without and special topolygy handing procedures added to the scheme. This permits synchronously extracting several anatomical structures. The experiments on some medical images obtained from different medical imaging methods demonstrate that the proposed approach is competent for medical image segmentation.

Key words medical image segmentation, geometric active contour, multi-scale, level Set theory.

一种新的用于医学图像分割的几何活动轮廓模型 *

岑 峰 戚飞虎

(上海交通大学计算机科学与工程系，上海，200030)

摘要 提出一种新的几何活动轮廓模型对医学图像进行分割. 首先，我们对几何活动轮廓模型中吸引力场进行正则化，扩大目标轮廓边缘对的轮廓曲线的吸引力范围，增加轮廓曲线搜寻凹轮廓的能力. 然后，采用多尺度模型增加对边缘提取的精确度. 将正则化方法与多尺度方法相结合，能够很好的抑制医学图像中的噪声和虚假边缘的干扰. 这一方法能够在不采用任何附加拓扑控制的情况下自动控制轮廓曲线的拓扑结构变化，同时提取多个解剖结构. 对来自不同成像技术的医学图像的分割，结果表明该方法是一种有效的医学图像分割方法.

关键词 医学图像分割，几何活动轮廓，多尺度，Level Set 理论.

Introduction

Computerized image segmentation has played an increasingly important role in medical image analysis, and has widely used in surgical planning, navigation, simulation etc. Segmenting anatomical structure from medical images such as CT, MR, PET etc. is difficult due to the complexity and variability of the anatomic shape of interest and corraption of the image caused by noise and sampling artifacts.

Active contour[4] is a promising and vigorously researched boundary finding segmentation approach. This method has been widely used in medical image segmentation with promising result, since it offers robustness to both image noise and boundary gaps. However, traditional active contour is difficult to adapt the model topology such as splitting or emerging without any additional topology-controlling scheme.

Geometric active contours moel, introduced in [1-3] as a geometric alternative for traditional active contour or ‘snake’ to naturally handle the topological changes of the evolving contour, extensively studied recently[4,6,10~12]. This model based on curve evolution theory and level set method, involves solving the ener-

* The project supported by National Natrual Science Foundation of China (No. 60072029)

Received 2003 - 01 - 14, revised 2003 - 04 - 14

* 国家自然科学基金(批准号 60072029)资助项目

稿件收到日期 2003 - 01 - 14，修改稿收到日期 2003 - 04 - 14

gy-based minimization problem by the computation of geodesic or minimal distance curves. In this approach, a curve is represented implicitly as a level set of a higher dimensional scalar function.

Although the geometric active contour model has such advantages over the snake, it has many drawbacks. This method is sensitive to the starting position of the contour and the noise and difficult to deform a contour into the boundary concavities, and allows the contour leaking through the gaps of the concept contour and the weak edges as well. These drawbacks cause diffculties when using the geometric active contour to segment the complicated medical image segmentation.

To solve these problems, we extend the geometric active contours by regularizing the edge attraction force field and using a multi-scale segmentation scheme. These extensions are able to increase the boundary capture range, and encourage the robustness to the noise and the spurious edges.

1 Geometric Active Contours Model

Geometric active contour was proposed independently by Caselles et al. [1,2] and Kichenassamy et al[3]. The formulation of Geometric Active Contours is based on curve evolution theory and Level Set method. The topological changes of the curve are naturally handled, which allows detection of allows detection of all objects that appear in the image plane without knowing their exact number.

1.1 Dynamic Models

Let $I:[0,a]\times[0,b]\rightarrow R^{+}$ be a given image in which we want to detect the objects boundaries. As an energy minimizing approach, the Geometric Active contours evolve the curve C to minimize an objective curve energy function. To minimize the curve energy is equivalent to searching for steady state solution of the following Euler-Lagrange equation[1]:

$$\frac{\partial C}{\partial t} = g(I)(\kappa + V_0)\vec{N} - (\nabla g(I)\cdot\vec{N})\vec{N}, \qquad (1)$$

Where κ denotes the Euclidean curvature, $\vec{N}$ denotes the unit inward normal, V_0 is a constant, $g(I)$ is a positive edge indicator function that depends on the image, and gets small value along the edges and higher value elsewhere. In this paper, we use the following form of $g(\Box)$,

$$g(h(I)) = e^{-|h(I)|l}, \qquad (2)$$

Where l is a positive real constant, $h(I)$ is the edge detecor, which is defined by:

$$h(I(x,y)) = \begin{cases} |\nabla[G_\sigma(x,y)*I(x,y)]|^2 & \text{step edges} \\ |G_\sigma(x,y)*I(x,y)|. & \text{line edges} \end{cases} \qquad (3)$$

Where G_σ denotes a 2-D Gaussian function with standard deviation σ.

According to curve evolution theory, $\frac{\partial C}{\partial t} = \kappa\vec{N}$ is the Euclidean shortening flow, which will smooth a curve, eventually shrinking it to a circular point; $\frac{\partial C}{\partial t} = V_0\vec{N}$ is the gradient flow, which will locally minimize the area enclosed by C, where V_0 is a coefficient determining the speed and direction of deformation. Among the first term at the right of equation (1), $g(I)$ is a multiplicative stopping term. If objects have good contrast, the curve evolution will stop at the boundary of objects, since $g(I)$ approximates zero along the boundary. However, when the object boundary is weak or indistinct, $g(I)$ does not vanish along the boundary, and the curve continues its propagation and may ship its desired location. The second term at the right of equation (1) may partially remedy this problem. In this term, $\nabla g(I)$ is an edge attraction force, which points towards the middle of the boundaries. When the curve pass the boundary, $-(\nabla g(I)\cdot\vec{N})\vec{N}$ pulls it back, and finally stops the curve at the desired position, where the residual force corresponding to the first term at the right of equation (1) can be counteracted.

The evolution of the curve is implemented by level set method proposed by Osher Sethian. [7]

1.2 Level Set Method

The Osher Sethian[7] level set method provides the numerical scheme for geometric deformable models. A useful property of this approach is that the level set function remains a valid function while the embedded curve can change its topology.

Now, Let $\psi(x,y,t):\mathrm{R}^2\rightarrow\mathrm{R}$ be a level set function with the cure $C(t)$ as its zero level set. We have $C(t)=\{(x,y):\psi(x,y,t)=0\}$. A common choice of ψ is to set $\psi(x,y,t)=d(x,y)$, where $d(x,y)$ is a signed distance from the grid point (x,y) to the surve C, with negative sign in the interior and positive in the exterior of the closed curve.

According to level set method, the corresponding geometric active contour model written in its level set formulation is given by,

$$\frac{\partial\psi}{\partial t} = g(I)(\kappa + V_0) | \nabla\psi | + \nabla g(I) \cdot \nabla\psi, \quad (4)$$

where the curvature κ is given by,

$$\kappa = \frac{\psi_{xx}\psi_y^2 - 2\psi_x\psi_y\psi_{xy} + \psi_{yy}\psi_x^2}{(\psi_x^2 + \psi_y^2)^{3/2}}, \quad (5)$$

where ψ_a denotes $\frac{\partial\psi}{\partial a}$, ψ_{ab} denotes $\frac{\partial^2\psi}{\partial a\partial b}$.

2 Edge Attraction Field Regularization

In order to increase the capture range of an active contour for the traditional active contour models, Chengyand Xu *et al.* [8,9] proposed a new external force, GVF (Gradient Vector Flow), which is computed as the regularization of image force. Similarly, in geometric active contour models, we regularize the edge attraction field to smoothly increase the capture range of the object boundaries.

Assuming that the regularized edge attraction field is $Q(x,y) = (p(x,y), q(x,y))$, $Q(x,y)$ is given by minimizing the following energy functional

$$\varepsilon = \iint \mu(| \nabla g |) | \nabla Q |^2 + (1 - \mu(| \nabla g |)) | Q + \nabla g |^2 \mathrm{d}x\mathrm{d}y. \quad (6)$$

The first term within the integrand is referred to as the smoothing term, since this term alone will produce a smoothly varying field. The second term is referred to as the data term, since it encourages Q to be close to $-\nabla g$. The parameter $\mu(|\nabla g|)$ with the variable of $-\nabla g$ is a regularization parameter governing the trade-off between the first term and the second term.

Since we want Q to be slowly varying at the location far from the edges, but to conform to $-\nabla g$ near the edges, $\mu(\square)$ should grow larger away from the edges, whereas, $\mu(\square)$ should become smaller near the edges. Therefore, we use the following weighting function

$$\mu(| \nabla g |) = \exp(-k | \nabla g |^2). \quad (7)$$

Where k is a positive real constant.

According to ref. [9], the regularized edge attraction force field can be found by treating p and q as functions of time, and searching the equilibrium slution of following diffusion equations

$$\begin{cases} \frac{\partial p}{\partial t} = \mu(| \nabla g |) \nabla^2 p - (1 - \mu(| \nabla g |))(p + g_x) \\ \frac{\partial q}{\partial t} = \mu(| \nabla g |) \nabla^2 q - (1 - \mu(| \nabla g |))(q + g_y). \end{cases} \quad (8)$$

Where g_x and g_y denote the component of ∇g in the direction of x coordinate and y coordinate, respectively.

There are two advantages for using the regularization approach. First, this approach increases the capture range of edge attraction force field. Furthermore, regularization also could fill the gaps of the broken boundary with the edge attraction field pointing towards the subjective contour. Fig. 1 shows a streamline example depicting the regularized edge attraction force field, in which regularization was applied to a simulated image containing an object that has both gaps (indicated by A) and concavity.

Second, regularization is able to smooth the edge attraction force field, and reduce the effects of the noise and the spurious edges. Note that, in image plane, the edge attraction force associated to noises and spurious edges is relatively small. Since μ is a monotonically non-increasing function of k, in order to suppress noises and spurious edges through the regularization approach, we could tune the parameter k in equation (7) to make μ become considerable larger near the noise and the spurious edge than that near the object boundary.

After compute $Q(x,y)$, we replace the edge attraction force field in equation (1) by $Q(x,y)$, yielding

$$\frac{\partial C}{\partial t} = g(I)\kappa\vec{N} + \gamma(Q \cdot \vec{N})\vec{N}, \quad (9)$$

and the corresponding level set formulation

$$\frac{\partial\psi}{\partial t} = g(I)\kappa | \nabla\psi | - \gamma Q \cdot \nabla\psi. \quad (10)$$

Note that in equation (1), (9), we not only replace ∇ g with $-Q$, but also multiply the second term by γ, which is a positive real constant, to adjust the proportion between the elastic force and the attraction force. Furthermore, comparing (1), (4) with (9), (10), we also omit pressure force, because the at-

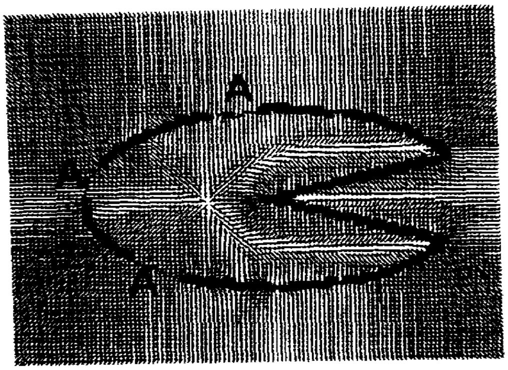

Fig. 1 Streamlines of regularization attraction field
图1 正规化吸引力场流线示意

traction range of regularization force field is large enough to capture the initial curve far from the boundaries.

3 Multi-scale Model

In order to increase the robustness of the model to the noise, we use a large σ in the Gaussianfilter in our model proposed above, for the large-scale filter can effectively smooth the noisy image data. Nonetheless, the large-scale filter has the effect of blurring the edges, which will force the curve convergence to inaccurate boundary, leading to an unreliable result. Fig 2 (a) illustrates the position shift of the edge in one dimension due to large-scale edge detector. The edge position (point B) detected by employing a large-scale edge detector shifts away from that (point A) detected by employing a small-scale edge detector. Furthermore, the regularization of the attraction force field enlarges the shift. We notice that the local minimum of $|\nabla g|$ exists at the edge, while the local maximum of $|\nabla g|$ is in the proximity of the edge. When the filter scale σ increases, the position of the local maximum magnitude of the edge attraction force becomes away from the boundary. From preceding discussion, we know that the regularization field is computed as a diffusion of the gradient vector of g, which extends the vector from the great intensity regions to small intensity and homogeneous regions smoothly without any change of the vector direction. Because the gradient vectors near the edge are all directed towards the middle of the edge, the direction of the diffusion at different side of the edge are opposite. In the regularizing attraction force field, the detected edge is at the position where the opposite diffusions can counteract each other, and the directions of the force vectors at different side of the detected edge are opposite. Now, if the gradient vectors at both sides of the edge have same magnitude, the opposite diffusion would counteract each other at the edge, and the regularizing force vectors point towards the edge. However, if the magnitudes are different, the diffusion of ∇g at each side of the edge is not able to counteract each other along the real edge. Here, we refer the real edge to the edge detected by the edge detector in the image, i. e. the edge in the attraction force field before regularizing. Thus, the detected edge

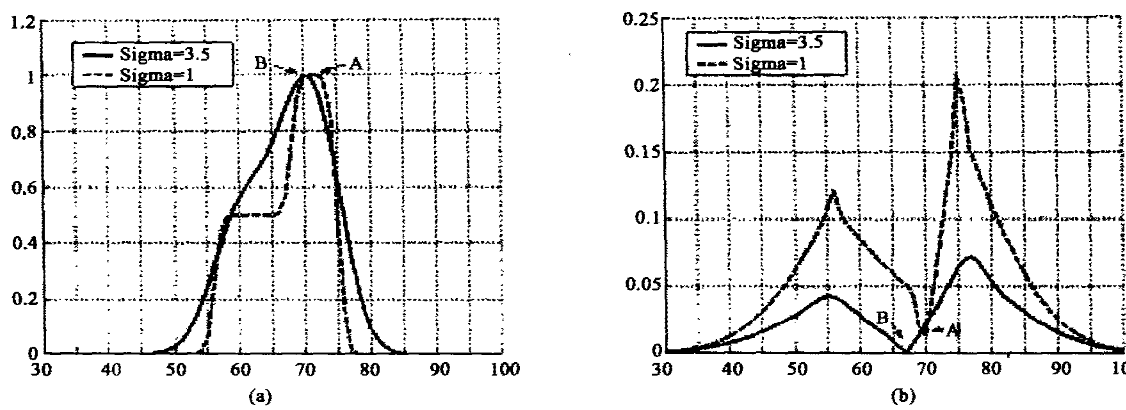

Fig. 2 Edge shift in one dimension (a) detected edge position and intensity using different scales of edge detector (b) the intensity of regularization attraction force field corresponding to Fig. 2(a). A and B denote the edge position with $\sigma = 1$ and $\sigma = 3.5$, respectively
图2 一维情况下边缘点发生偏离情况(a)采用不同尺度边缘检测算子得到的边缘位置(b)与图(a)相对应的边缘检测算子所得的正则化边缘吸引力场强度. 图中 A,B 分别为 $\sigma = 1$ 和 $\sigma = 3.5$ 时对应的边缘位置

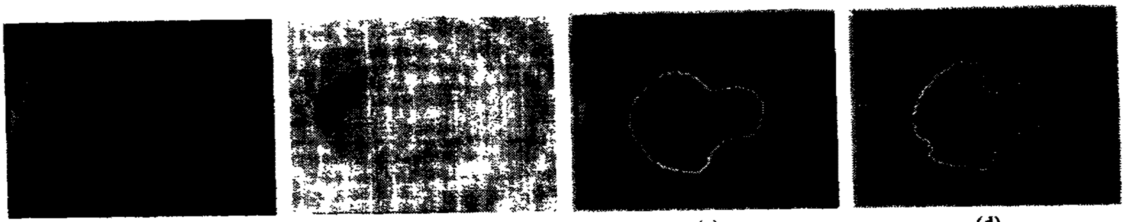
(a) (b) (c) (d)

Fig. 3 Segmentation of the left ventricle of a human heart (short-axis section) (a) The MR image (b) The streamlines of regularization attraction force field with $\sigma = 3$ (c) Initial (dot curve) and intermediate contour (white curve) with $\sigma = 3$ (d) Final contour with $\sigma = 1$
图 3 对人的心脏左心室(短轴部分)进行分割(a) MR 原图像(b) $\sigma = 3$ 时正规化吸引力场流线示意(c) $\sigma = 3$ 时的初始区线(点)和中间结果(白线)(d)最终结果, $\sigma = 1$

in the regularizing attraction force field shifts towards the side of the real edge where the magnitude of $|\nabla g|$ is lower. We see this effect in Fig. 2(b). The shift of A away from B in Fig. 2(b) is larger than that in Fig. 2(a).

To solve this problem, we introduce the multi-scale technique. The multi-scale technique can effectively reduce the sensitive to the noise and the spurious edge, and improve the accuracy of boundary detection. First, we regularize the gradient vector of g which is derived from emplying large-scale σ. Because the regularizing attraction force field that is dervied from using large-scale σ is insensitive to the noise data and has larger capture range, the initializing curve could be far away from the object boundary. In the large-scale, the curve evolution may stop in the proximity of the boundary rather that accurately along the boundary, so we need reduce the scale of σ to improve the contour accuracy. Second, we reduce the scale of σ gradually, and regularize the attraction force field associated to the small σ again. Using the result of last step as the initializing curve, we evolve the curve. Then we reduce the scale of σ again, and repeat the second step until σ is equal to the smallest scale. After the first step, the purpose of regularization is reducing the noises near the boundary and improving the accuracy of boundary detection. It means that the extension of the attraction range is unnecessary and the convergence of equation (8) need not be achieved. Thus, We only iterate the enough constant times in equation (8) so that the nose near the object boundary can be suppressed.

4 Experimental Result

We have tested our algorithm on several real medical images, including CT, MRI, and physical cross-sectional data. All experiments start at the large-scale $\sigma = 3$, and gradually decrease σ with a step $\Delta\sigma = 0.5$, then obtain the final results at $\sigma = 1$.

Fig. 3 shows the extraction of the inner wall of the left ventricle from a noisy MR image. The original image and the streamlines of the regularizing attraction force field with $\sigma = 3$ are shown in Fig. 3(a) and 3(b), respectively. We initialized the contour across the inner wall of ventricle, as the dot rectangle shown in Fig. 3(c), an intermediate extraction result with large-scale edge detector, $\sigma = 3$, is also shown. The result shows that the contour finds the boundary of inner wall approximately in the presence of both boundary concavities and convexities. The final result using the multi-scale scheme is shown in Fig. 3(d). Comparing Fig. 3(c) with Fig. 3(d), we note that the result obtained through the multi-scale scheme at small-scale is more accurate than that obtained at large-scale. Therefore, the multi-scale scheme can improve the segmentation accuracy.

We also applied the proposed contour model on the CT image of leg to segment two object, fibula and tibia, synchronously as shown in Fig. 4. Note that, in Fig. 4 (a), the initial curve (the dot rectangle) is far from the object boundary and the CT image is noisy and contains many spurious edges of the muscle between the initial curve and the fibula and tibia. However, the regu-

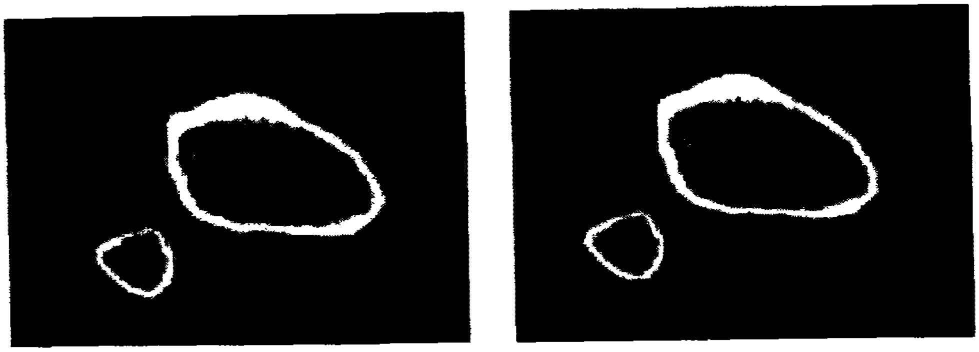

(a) (b)

Fig. 4 Segmentation of the fibula and the tibia on CT image of human leg (a) Searching procedure with $\sigma = 3$ (b) Final contour with $\sigma = 1$

图4 对腓骨 CT 图的分割(a)$\sigma = 3$ 时的搜索过程(b)$\sigma = 1$ 时的最终结果

larization method effectively reduces the effects of these spurious edges and extends the attraction range of the object boundary. Eventually, the regularizing attraction force field deforms the contour into the proximity of the bone boundary. In Fig. 4(a), the white solid curve shows the intermediate result with $\sigma = 3$. Then we gradually decreased the scale and obtained the final accurate result in Fig. 4(b) with $\sigma = 1$.

5 Conclusion

We have introduced new extensions to the geometric active contour. These extensions include regularizing the attraction force field and the multi-scale scheme. The regularization of the attraction force field, suppressing the noise and spurious edges and extending the capture range of the boundary, allows for flexible initialization of the contour and encourages to convergence concavities. Furthermore, the multi-scale scheme not only reduces the noise, but also improves the accuracy of the segmentation. The experiments on different medical images demonstrate that the proposed method is a competent approach for medical image segmentation.

To improve the performance and automation of segmentation, further investigation into optimal selection of some parameters such as γ, k is desirable. In addition, since the level set implementation is computationally expensive, finding a fast algorithm is also the work direction.

REFERENCES

[1] Gaselles V, Kimmel R, Sapiro G. Geodesic active contours. *Int. J. Computer Vision*, 1997, **22**: 61—79

[2] Caselles V, Catte F, Coll T. *et al*. A greometric model for active contours. *Numerische Mathematik*, 1993, **63**: 1—31

[3] Kichenassamy A, Kumar A, Olver P. *et al*. Gradient flows and geometric active contour models. *In IEEE Int'l Conf. Comp. Vision*, 1995: 810—815

[4] Malladi R, Sethian J A, Vemuri B C. Shape modeling with front propagation: a level set approach. *IEEE T. Patt. Anal. Mach. Intell.*, 1995, **17**: 158—175

[5] Kass M, Witkin A, Terzopoulos D. Snakes: Active Contour Models: *Int. J. Computer Vision*, 1987, **1**(1): 321—331

[6] Siddiqi K, Lauziere Y B, Tannenbaum A. *et al*. Area and length minimizing flows for shape segmentation. *IEEE T. Imag. Proc.*, 1998, **7**: 433—443

[7] Osher S, Sethian J A. Fronts propagating with curvature-dependent speed: Algorithms based on hamilton-jacobi formulation. *J. Comp. Physics*, 1988, **79**: 12—49

[8] Xu C, Prince J L. Snake, shape, and gradient vector flow. *IEEE Trans. Pattern Anal. Machine Intell.*, 1998, **7**(3): 359—369

[9] Xu C, Prince J L. Generalized gradient vector flow external forces for active contours. *Signal Processing*, 1998, **71**: 131—139

[10] Goldenberg R, Kimmel R, Rivlin E, *et al*. Fast Geodesic Active Contours. *IEEE Transactions on Image Processing*, 2001, **10**(10): 1467—1475

[11] Paragios N, Deriche R. Geodesic active contours and level sets for the detection and tracking of moving objects. *IEEE Transactions on Pattern Analysis and Machine Intelligence*. 2000, **22**: 266—280

[12] Leventon M E, Grimson W E L, Faugeras O. Statistical shap influence in geodesic Active Contours. *CPVR* 2000, **1**: 316—323